

<b>UK EPR</b>	Title: PCSR – Sub-chapter 4.4 – Thermal and hydraulic design	
	<b>UKEPR-0002-044 Issue 04</b>	
Total number of pages: 53		Page No.: I / IV
Chapter Pilot: D. PAGE BLAIR		
Name/Initials <i>D. Page Blair</i> Date 29-06-2012		
Approved for EDF by: A. PETIT		Approved for AREVA by: G. CRAIG
Name/Initials <i>A. Petit</i> Date 19-07-2012		Name/Initials <i>G. Craig</i> Date 19-07-2012

### REVISION HISTORY

Issue	Description	Date
00	First issue for INSA information.	04-01-2008
01	Integration of technical and co-applicant review comments.	29-04-2008
02	PCSR June 2009 update: <ul style="list-style-type: none"> <li>– Clarification of text</li> <li>– Inclusion of references</li> <li>– Design evolutions to account for December 2008 design freeze (Primary flow rates and temperatures, fuel melting temperature ...)</li> </ul>	26-06-2009
03	Consolidated Step 4 PCSR update: <ul style="list-style-type: none"> <li>– Minor editorial changes</li> <li>– Clarification of text</li> <li>– Inclusion and update of references</li> <li>– Inclusion of information on nucleate boiling (new §1.4), crud deposition (§2.2.6) and critical heat flux (§2.2.7).</li> </ul>	26-03-2011
04	Consolidated PCSR update: <ul style="list-style-type: none"> <li>- References listed under each numbered section or sub-section heading numbered [Ref-1], [Ref-2], [Ref-3], etc</li> <li>- Minor editorial changes</li> <li>- Clarification added regarding validity of conclusions (§2.2.7)</li> <li>- Reference updated to English document (§2.6.2)</li> </ul>	19-07-2012

Text within this document that is enclosed within curly brackets "{...}" is AREVA or EDF Commercially Confidential Information and has been removed.

<b>UK EPR</b>	Title: PCSR – Sub-chapter 4.4 – Thermal and hydraulic design	
	<b>UKEPR-0002-044 Issue 04</b>	Page No.: II / IV

Copyright © 2012

**AREVA NP & EDF  
All Rights Reserved**

This document has been prepared by or on behalf of AREVA NP and EDF SA in connection with their request for generic design assessment of the EPR™ design by the UK nuclear regulatory authorities. This document is the property of AREVA NP and EDF SA.

Although due care has been taken in compiling the content of this document, neither AREVA NP, EDF SA nor any of their respective affiliates accept any reliability in respect to any errors, omissions or inaccuracies contained or referred to in it.

All intellectual property rights in the content of this document are owned by AREVA NP, EDF SA, their respective affiliates and their respective licensors. You are permitted to download and print content from this document solely for your own internal purposes and/or personal use. The document content must not be copied or reproduced, used or otherwise dealt with for any other reason. You are not entitled to modify or redistribute the content of this document without the express written permission of AREVA NP and EDF SA. This document and any copies that have been made of it must be returned to AREVA NP or EDF SA on their request.

Trade marks, logos and brand names used in this document are owned by AREVA NP, EDF SA, their respective affiliates or other licensors. No rights are granted to use any of them without the prior written permission of the owner.

#### Trade Mark

EPR™ is an AREVA Trade Mark.

#### For information address:



AREVA NP SAS  
Tour AREVA  
92084 Paris La Défense Cedex  
France



EDF  
Division Ingénierie Nucléaire  
Centre National d'Équipement Nucléaire  
165-173, avenue Pierre Brossolette  
BP900  
92542 Montrouge  
France

<b>UK EPR</b>		
	Title: PCSR – Sub-chapter 4.4 – Thermal and hydraulic design	
	<b>UKEPR-0002-044 Issue 04</b>	Page No.: III / IV

## TABLE OF CONTENTS

- 0. SAFETY REQUIREMENTS**
  - 0.1. SAFETY FUNCTIONS**
  - 0.2. FUNCTIONAL CRITERIA**
  - 0.3. DESIGN REQUIREMENTS**
  - 0.4. TESTING**
- 1. DESIGN BASIS**
  - 1.1. DEPARTURE FROM NUCLEATE BOILING DESIGN BASIS**
  - 1.2. FUEL TEMPERATURE DESIGN BASIS**
  - 1.3. CORE FLOW DESIGN BASIS**
  - 1.4. NUCLEATE BOILING**
  - 1.5. HYDRODYNAMIC STABILITY DESIGN BASIS**
- 2. DESCRIPTION OF LIMITING PHYSICAL PHENOMENA - DESIGN CRITERIA**
  - 2.1. SUMMARY**
  - 2.2. CRITICAL HEAT FLUX RATIO OR DEPARTURE FROM NUCLEATE BOILING RATIO AND MIXING TECHNOLOGY**
  - 2.3. HEAT FLUX AND LINEAR POWER DEFINITIONS**
  - 2.4. HEAT TRANSFER AND VOID FRACTION CORRELATIONS RADIAL POWER DISTRIBUTION**
  - 2.5. HYDRODYNAMIC INSTABILITY**
  - 2.6. REACTOR VESSEL AND CORE HYDRAULICS**
  - 2.7. THERMAL EFFECTS OF OPERATIONAL TRANSIENTS**
  - 2.8. UNCERTAINTIES**

<b>UK EPR</b>		
	Title: PCSR – Sub-chapter 4.4 – Thermal and hydraulic design	
	<b>UKEPR-0002-044 Issue 04</b>	Page No.: IV / IV

### **3. OPERATING THERMAL AND HYDRAULIC REACTOR PARAMETERS**

**3.1. TEMPERATURE POWER OPERATING MAP**

**3.2. THERMAL AND HYDRAULIC CHARACTERISTICS**

### **4. ANALYSIS METHODS AND DESIGN DATA**

**4.1. METHODOLOGY USED FOR TRANSIENT ANALYSIS**

**4.2. INFLUENCE OF POWER DISTRIBUTION**

**4.3. CORE ANALYSIS TOOLS**

**4.4. THERMAL RESPONSE OF THE CORE**

**4.5. HYDRAULICS DATA**

**4.6. HYDRODYNAMIC INSTABILITY**

### **5. TESTING AND VERIFICATION**

**5.1. TESTS PRIOR TO INITIAL CRITICALITY**

**5.2. INITIAL POWER AND PLANT OPERATION**

**5.3. COMPONENT AND FUEL INSPECTIONS**

### **6. INSTRUMENTATION REQUIREMENTS**

**6.1. LOW DNBR FUNCTIONS**

**6.2. HIGH LINEAR POWER DENSITY (HLPD) FUNCTIONS**

**6.3. FIXED IN CORE NEUTRONIC INSTRUMENTATION**

**6.4. AEROBALL MEASURING SYSTEM (AMS)**

**6.5. EXCORE NEUTRONIC INSTRUMENTATION**

## **SUB-CHAPTER 4.4 – THERMAL AND HYDRAULIC DESIGN**

### **0. SAFETY REQUIREMENTS**

#### **0.1. SAFETY FUNCTIONS**

The safety functions carried out by thermal and hydraulic design are:

- Removal of heat produced in the fuel via the coolant,
- Containment of radioactive substances (actinides and fission products) within the first barrier.

#### **0.2. FUNCTIONAL CRITERIA**

##### **0.2.1. Controlling core reactivity**

This has no impact on the thermal-hydraulic design.

##### **0.2.2. Removal of heat produced in the fuel**

The thermal and hydraulic design must enable the removal of heat produced in the core by maintaining an efficient heat transfer between the fuel rod and the coolant fluid under normal and incident operating conditions.

##### **0.2.3. Containment of radioactive products**

The lack of departure from nucleate boiling under incident operating conditions ensures that the integrity of the fuel cladding is not compromised.

#### **0.3. DESIGN REQUIREMENTS**

The safety functions related to thermal and hydraulic design require the application of a quality assurance program whose aim is to document and monitor activities related to design.

#### **0.4. TESTING**

##### **0.4.1. Pre-operational tests**

The underlying features of the selected scenarios in the safety analyses must be checked during the first physical core tests. Some of these tests, such as verification of the reactor coolant flow rate or the drop time of the Rod Cluster Control Assembly (RCCA), are carried out regularly. Other tests are only carried out in full on commissioning of a lead unit.

For subsequent units, only those tests are performed that are needed to ensure that the thermal-hydraulic characteristics of the core are identical to those of the core in the lead unit.

#### **0.4.2. In-service monitoring**

The reactor coolant flow rate and the RCCA drop time must be measured regularly.

#### **0.4.3. Periodic tests**

Not applicable.

## **1. DESIGN BASIS**

The overall objective of the thermal and hydraulic design of the reactor core is to provide heat transfer that is compatible with the heat generation distribution in the core, such that heat removal by the reactor coolant system or the safety injection system (when applicable) ensures that the requirements presented in section 0 are met.

In order to satisfy these criteria, the following design bases have been established for the thermal and hydraulic design of the reactor core.

### **1.1. DEPARTURE FROM NUCLEATE BOILING DESIGN BASIS**

There must be at least a 95% probability at a 95% confidence level that Departure from Nucleate Boiling (DNB) will not occur on the limiting fuel rods during normal operation and operational transients, and any transient conditions arising from faults of moderate frequency (PCC-1 and PCC-2 events).

By preventing DNB, adequate heat transfer is ensured between the fuel cladding and the reactor coolant, thereby preventing cladding damage as a result of inadequate cooling. Maximum fuel rod surface temperature is not a design basis, as it will be within a few degrees of coolant temperature during operation in the nucleate boiling region. Limits provided by the nuclear control, limitation, and protection systems are such that this design basis will be met for transients associated with PCC-2 events. There is an additional Departure from Nucleate Boiling Ratio (DNBR) (see section 2.2.2) margin at rated power operation and during normal operating transients.

The use of simplified DNBR on-line calculations in the protection system and in the surveillance system enables the design criterion to be met by defining a low DNBR Reactor Trip ( $DNB_{RT}$ ) and a Limiting Condition of Operation ( $DNB_{LCO}$ ) with regard to DNB, directly based on the derived variable representative of the phenomenon to avoid.

The on-line calculated values are provided by systems that use measurements with an algorithm to derive the local conditions and apply the chosen Critical Heat Flux (CHF) predictor to calculate the CHF.

The uncertainties in the derivation and the measurement accuracy are taken into account when establishing the setpoints for the on-line DNBR calculated value. The setpoints are set such that there is a 95% probability at a 95% confidence level that DNB will not occur when the DNBR on-line calculated value is equal to the DNBR thresholds.

## 1.2. FUEL TEMPERATURE DESIGN BASIS

During modes of operation associated with PCC-1 and PCC-2 events, there is at least a 95% probability at the 95% confidence level that the fuel rods with maximum linear power density (W/cm) will not exceed the fuel melting temperature.

The melting temperature of unirradiated  $\text{UO}_2$  is taken as 2810°C {CCI Removed}  
<sup>b</sup>. The melting temperature of unirradiated MOX depends on the Pu molar fraction (y) and is calculated with the following formula:

$$T_{\text{melting}}(^{\circ}\text{C}) = 2810 - 540y + 121y^2$$

{CCI Removed}

b

By precluding fuel melting, the fuel geometry is preserved and the possible adverse effects of molten fuel on the cladding are eliminated.

## 1.3. CORE FLOW DESIGN BASIS

A minimum of 94.5% [Ref-1] of the thermal flow rate will pass through the fuel rod region of the core and be effective for fuel rod cooling. Coolant flow through the guide thimbles, as well as the leakage from the core barrel-baffle region into the core is not considered effective for heat removal.

Core cooling analyses are based on the thermal flow rate (minimum flow) entering the reactor vessel. Under hot dome conditions, a maximum of 5.5% of this value is allotted as bypass flow. This includes rod cluster control guide thimble cooling flow, head cooling flow, baffle leakage, and leakage to the vessel outlet nozzle.

## 1.4. NUCLEATE BOILING

In order to prevent excessive corrosion rates and crud build up, a limiting value of 5% void fraction (hot channel) is retained for the determination of the maximum enthalpy rise  $F\Delta H$  [Ref-1]. This value is assessed conservatively using M5® worldwide experience, which demonstrates the good corrosion resistance of this material even in high duty plants with nucleate boiling up to 8%. This operating experience confirms the behaviour observed in out-of-pile tests and it shows that when heavy crud has been observed there was no impact on M5® corrosion thickness. For design purposes, this limiting value is applied for  $F\Delta H$  in nominal conditions using best estimate flow rate conditions.

## 1.5. HYDRODYNAMIC STABILITY DESIGN BASIS

Modes of operation associated with PCC-1 and PCC-2 events must not lead to hydrodynamic instability.

## 2. DESCRIPTION OF LIMITING PHYSICAL PHENOMENA - DESIGN CRITERIA

### 2.1. SUMMARY

Values of pertinent parameters along with DNB ratios, fuel temperatures, and linear heat generation rates are presented in Sub-chapter 4.4 - Table 1 for all coolant loops in service. The reactor is designed to ensure a minimum DNBR as well as no fuel centre line melting during normal operation, operational transients, and faults of moderate frequency.

### 2.2. CRITICAL HEAT FLUX RATIO OR DEPARTURE FROM NUCLEATE BOILING RATIO AND MIXING TECHNOLOGY

The minimum DNBR in the limiting flow channel will be downstream of the peak heat flux location (hot spot) due to the increased downstream enthalpy rise.

DNBRs are calculated by using the predictor and definitions described in sections 2.2.1 and 2.2.2. The FLICA III-F computer code, which is described in Appendix 4, is used to determine the flow distribution in the core and the local conditions in the hot channel for use in the DNB predictor.

#### 2.2.1. Departure from nucleate boiling technology

##### Critical Heat Flux (CHF) Predictor

Early experimental studies of DNB were conducted with fluid flowing inside single heated tubes or channels and with single annulus configurations with one or both walls heated. The results of the experiments were analysed using many different physical models of the DNB phenomenon, but all resultant predictors are highly empirical in nature.

As testing methods progressed to the use of rod bundles, instead of single channels, it became apparent that the bundle average flow conditions could not be used in DNB predictors. Test results showed that predictors based on average conditions were not accurate predictors of DNB heat flux. This indicated that knowledge of the local sub-channel conditions within the bundle was necessary.

In order to determine the local sub-channel conditions, the FLICA III-F computer code was developed. In this code, a rod bundle is considered to be an array of sub-channels each of which includes the flow area formed by four adjacent rods. The sub-channels are also divided into axial steps such that each may be treated as a control volume. The local fluid conditions in each control volume are calculated by solving simultaneously the mass, energy, and momentum equations. Critical heat flux is predicted using the sub-channel local fluid conditions calculated by the design code and the FC-CHF correlation [Ref-1].

##### Test data using for the FC-CHF correlation

The experimental basis for the FC-CHF correlation consists mainly of results of tests of AREVA fuel assemblies performed in the University of COLUMBIA loop and OMEGA loop in the CEN (Nuclear Research Centre) test facility in Grenoble [Ref-1].



The test bundle consisted of 25 heater rods in a 5 x 5 array supported by grids. These rods were spaced in a 12.6 mm mesh array and had an outside diameter of 9.5 mm. The rods were electrically heated. The rods located at the centre of the cluster were overheated to simulate a boiling crisis in that portion of the assembly. All rods were equipped with axially-mounted thermocouples to detect the onset of the boiling crisis.

The tests were performed with:

- Uniform axial flux distribution
- Non-uniform axial flux distribution
- Typical cells
- Guide thimble cells.

The tests were performed over the following parameter ranges:

- Pressure            20.7     <   P     <   170.6 bar.
- Mass velocity    930       <   G     <   4790 kg/m<sup>2</sup>/s.
- Quality            -0.22    <   X     <   0.44.

These ranges adequately encompass EPR operating conditions. Under nominal operating conditions at minimum DNBR, locally prevailing values are approximately:

- Pressure            = 155 bar.
- Mass velocity    = 3500 kg/m<sup>2</sup>/s.
- Quality            ~ -0.10.

Under accident conditions that are limiting in terms of DNBR, the following extreme values are anticipated at minimum DNBR

- Loss of flow accident                    G = 1500 kg/m<sup>2</sup>/s.
- Overheating                                X = 0.3.
- Steam line break (depressurisation)   P = 30 bar.

#### Uniform axial heat flux correlation form

The FC-CHF correlation is given in analytical form depending on:

- Thermal-hydraulic variables: pressure p, mass flow rate G and X,
- Fuel geometry, i.e. distances between grids,
- Cell type: differentiation between the two cell types, typical cell and guide thimble cell.

The main term of the correlation for uniform heat flux does not depend on the fuel geometry. It is only a function of the thermal-hydraulic variables. This term is assumed to depend linearly on X via the following relationship:

$$\Phi_{HCF} = A(p,G) - B(p,G)*X$$

The other terms related to the fuel depend on the following geometrical effects:

- Spacing between grids,
- Distance between the location of predicted critical heat flux and the location of the upstream grid.

The FC correlation has the following form:  $FCRIT(P,G,X,d_g,g_{sp},r_{tg})$

With:

$$FCRIT = a(P,G,X,d_g) + c(P,G,X,g_{sp}) + d(P,X,g_{sp},r_{tg})$$

{CCI Removed}

Non-uniform axial heat flux correlation form

The CHF values measured in a rod bundle with non-uniform axial flux distributions are lower, under the same local conditions, than those obtained from rod bundles with uniform distributions. Application of the CHF-correlation showed that the predicted flux was higher than the measured flux. The predicted value must therefore be corrected. This is achieved by applying the TONG non-uniform flux factor [Ref-2]. The corrected flux is expressed as:

$$\Phi = \frac{\Phi_U}{F_{NU}}$$

Where:

$\Phi$  is the corrected flux value

$\Phi_U$  is the predicted flux value for the uniform flux axial distribution.

$F_{NU}$  is the non uniform flux factor defined as:

$$F_{NU}(z^*) = \frac{C \int_0^{z^*} \phi(z) \exp(-C(z^* - z)) dz}{\phi(z^*) [1 - \exp(-C(z^*))]}$$

$z^*$  is the axial height of calculation,

$\phi(z)$  is the heat flux at height  $z$ ,

$\phi(z^*)$  is the flux calculated with a uniform Axial Flux Shape

$C$  is the coefficient whose dimension is inverse length, defined as:

$$C = \alpha (1 - X)^\beta G^\gamma$$

Where:

$X$  and  $G$  are the quality and mass velocity at the height of onset of boiling crisis;  $\alpha$ ,  $\beta$ , and  $\gamma$  are the following constants:

$$\alpha = 15.33 \text{ m}^{-1}$$

$$\beta = 7.15$$

$$\gamma = -0.35$$

with  $G$  in  $\text{kg/m}^2/\text{s}$ .

{CCI Removed}

{CCI Removed}

b

### 2.2.2. Definition of departure from nucleate boiling ratio

The Departure from Nuclear Boiling Ratio (DNBR), as applied to this design for both typical and thimble cold wall cells, is defined as:

$$\text{DNBR} = \frac{\Phi''_{\text{DNB,N}}}{\Phi''_{\text{loc}}}$$

Where:

$\Phi''_{\text{loc}}$  is the actual local heat flux

$$\Phi''_{\text{DNB,N}} = \frac{\Phi''_{\text{DNB,EU}}}{F}$$

$\Phi''_{\text{DNB,EU}}$  is the uniform critical heat flux as predicted by the FC-CHF correlation.

F is the TONG flux shape factor to account for non-uniform axial heat flux distributions.

### 2.2.3. Mixing effect between sub-channels

In a rod bundle, the flux channels formed by four adjacent fuel rods are open to each other through the gap between two neighbouring fuel rods. There is a cross-flow between channels because of the pressure differential between the channels.

The mixing effect reduces enthalpy rise in the hot channel.

The energy balance equation of the design code includes a term to model the turbulent enthalpy exchange between adjacent channels. This term is proportional to the enthalpy difference between adjacent channels and includes a Turbulent Mixing Coefficient.

The value of this coefficient is generally determined from a series of special tests on the type of grid assembly considered.

To decouple the EPR design from the fuel assembly as much as possible and to be conservative, a value lower than those established by tests is used: 0.043.

#### 2.2.4. Manufacturing uncertainties

Manufacturing uncertainties take into account the variations in fuel rod and fuel assembly materials and geometry arising during manufacture.

There are two kinds of manufacturing uncertainty:

- The effect of the pellet eccentricity and of the cladding ovalisation on the critical flux,
- The grid manufacturing tolerance impact on the critical flux.

These uncertainties are random. Thus, the penalties they induce may occur anywhere in the core and the co-location of the penalty due to the manufacturing tolerance and the local thermal-hydraulic conditions unfavourable to DNBR is also random.

##### a) Effect of the pellet eccentricity and of the cladding ovalisation on the critical flux

Some pellets may be eccentric with respect to the cladding at the start of life. Also, the cladding may ovalise with time. In these two cases, there is an azimuthal variation of the flux over a small axial distance.

In the case of an eccentric pellet, the local flux peak in a given angle extends axially over a distance of at most a few pellet lengths because of random contact between the pellets and the cladding at the start of life. This random character of the angle of contact is caused by variations in the shape of the ends of the pellets and by variations in the diameter of the pellets.

In the case of ovalised cladding, the local flux peak in a given angle extends axially over a distance of at most a few pellet lengths, taking into account the random azimuthal distribution of the fragments of the cracked pellet.

The hot channel uncertainties take into account the fact that the geometry and the materials of the rod and the assembly are not perfect.

Two hot channel uncertainties are taken into account; the heat flux engineering hot channel uncertainty and the engineering uncertainty applied to the nuclear enthalpy rise of the hot channel.

- Heat flux engineering hot channel uncertainty ( $F_Q^E$ ).

This uncertainty is used to evaluate the maximum local power peak (the hot spot) and is determined by statistically combining the tolerances for the fuel pellet diameter, density and enrichment.

Based on AREVA experience as a fuel supplier, this uncertainty is initially characterised by a normal distribution {CCI Removed} covering both UO<sub>2</sub> and MOX fuel. For each fuel reload it is confirmed that the actual value is lower than this decoupling value.

However, critical heat flux tests to determine the peak azimuthal heat flux over a 15 cm length have shown that it is not necessary to take into account this particular uncertainty in the local flux.

As 15 cm corresponds to around 10 pellet lengths, it is considered that the allowances for the effect of diameter, density, and enrichment on local heat generation rate do not decrease the DNBR.

Consequently, it is concluded that uncertainties in the flux peaking do not need to be taken into account.

- Engineering uncertainty applied to the nuclear enthalpy rise of the hot channel ( $F_{\Delta H}^E$ )

This uncertainty is determined by statistically combining the effects on the enthalpy rise of manufacturing tolerances for fuel density, fuel enrichment, and rod position.

Based on AREVA experience as a fuel supplier, this uncertainty is initially characterised by a normal distribution {CCI Removed}  
<sup>b</sup> covering both UO<sub>2</sub> and MOX fuel

For each fuel reload it is confirmed that the actual value is lower than this decoupling value.

- b) Effect of the grid manufacturing tolerances on the critical flux ( $F_{LC}^E$ )

This uncertainty directly represents the grid manufacturing tolerance impact on DNBR values. More precisely, it represents the impact of the grid pressure loss coefficient uncertainties due to manufacturing tolerances on core flow redistribution.

For fuel assemblies of the same design, the impact on the variability in DNBR values is negligible.

### 2.2.5. Effects of in-pile rod bow on critical heat flux

DNB can be influenced by the rod bow phenomenon which has been detected in examinations of irradiated assemblies. This phenomenon consists of rod displacement from its nominal position within a channel. It is strongly fuel dependent and the methodology described below is derived from the French experience.

The induced change in flow geometry implies a reduction in the CHF at which DNB occurs.

The DNBR rod bow penalty is quantified by a convolution of two models:

- A bounding relationship specifying the rod bow magnitude, i.e. channel closure as a function of fuel burn up based upon rod bow measurements of irradiated AREVA 17x17 fuel assemblies. This bounding relationship is given in Sub-chapter 4.4 - Figure 1.
- An expression relating the DNBR penalty to the closure of the channel, which was approved by the Nuclear Regulatory Commission (NRC) in 1979. It requires differentiation between full flow rate operation and reduced flow rate operation. The DNBR penalty as a function of channel closure used in the design is given in Sub-chapter 4.4 - Figure 2.

Tests have shown that no rod bow effect exists at low pressures but the effect is higher when the flow rate decreases.

The resulting model gives the DNBR penalty as a function of fuel burn up.

Based on AREVA fuel experience, under a burnup value of around 16,000 MWd/t there is no rod bow penalty. Above this value the penalty linearly increases but may be limited when rod burnup increases. Previous analyses have indicated that beyond a burnup of around 35,000 MWd/t, rods no longer have the maximum value of nuclear  $F\Delta H$ .

After analysing the  $F\Delta H$  decrease with burnup in the EPR fuel management regimes, the burnup limit used in assessing the rod bow penalty is 40,000 MWd/t.

{CCI Removed}

This describes the way the rod bow is presently considered for the EPR design. The actual application will depend on the actual fuel characteristics.

#### **2.2.6. Effect of crud deposition [Ref-1]**

{CCI Removed}

#### **2.2.7. Critical heat flux at the edge of the fuel assemblies [Ref-1]**

{CCI Removed}

### 2.3. HEAT FLUX AND LINEAR POWER DEFINITIONS

The core average and maximum heat flux and linear power are given in Sub-chapter 4.4 - Table 1. The methods of determining these quantities are given in section 3 of Sub-chapter 4.3.

### 2.4. HEAT TRANSFER AND VOID FRACTION CORRELATIONS RADIAL POWER DISTRIBUTION

The flow model used is based on a two phase flow model (Sub-chapter 4.4 - Figure 3) which takes into account thermal non-equilibrium for the liquid phase and unequal velocities of the liquid and vapour phases. The model is derived from mass, momentum, and energy balance equations for a turbulent two-phase flow. The liquid phase enthalpy balance equation allows sub-cooled boiling calculations. To close this set of equations, physical models of phase interactions, turbulent mixing, and fluid-wall interactions are required. These closure relationships are:

- A wall friction model
- A heat transfer model
- A velocity slip ratio model to take into account different velocities for the liquid and steam phases
- Turbulent viscosity and diffusivity coefficients, which are calculated from a model which includes mixing effects.

The reference sub-channel code FLICA III-F (see Appendix 4), which has its own heat transfer and void fraction models, is used for EPR core thermal-hydraulic design analysis, and more precisely to compute the local fluid properties needed to predict critical heat flux margins.

### 2.5. HYDRODYNAMIC INSTABILITY

Boiling flows may be susceptible to thermo-hydrodynamic instabilities. These instabilities are undesirable in reactors since they may cause a change in thermal-hydraulic conditions that may lead to a reduction in the DNB heat flux relative to that observed during steady flow condition. They may also induce potentially damaging vibration in core components. Consequently a thermal-hydraulic design criterion has been developed which states that modes of operation under PCC-1 and 2 events shall not lead to thermo-hydrodynamic instabilities.

Two specific types of flow instabilities are considered for PWR operation. These are the Ledinegg type of static flow instability and the density wave type of dynamic instability.

Ledinegg instability involves a sudden change in flow rate from one steady-state to another. This instability occurs when the derivative of the reactor coolant system pressure drop with respect to flow rate ( $\partial P/\partial G$  internal) is less than that of the loop supply (pump head) pressure drop with respect to flow rate curve ( $\partial P/\partial G$  external). The criterion for stability is thus  $\partial P/\partial G$  internal  $\geq$   $\partial P/\partial G$  external.

The mechanism of density wave oscillations in a heated channel can be described as follows. Briefly, an inlet flow fluctuation produces an enthalpy perturbation. This perturbs the length and the pressure drop of the single phase region and causes quality or void perturbations in the two-



phase region that travel up the channel with the flow. The quality and length perturbations in the two-phase region create two-phase pressure drop perturbations.

However, since the total pressure drop across the core is maintained by the characteristics of the fluid system external to the core, then the two-phase pressure drop perturbation feeds back to the single phase region. These resulting perturbations can be either attenuated or self-sustaining.

Hydrodynamic instability is further discussed in section 4.6.

## 2.6. REACTOR VESSEL AND CORE HYDRAULICS

### 2.6.1. Bypass flow

The coolant flow enters into the reactor vessel via the inlet nozzles. It then flows down through the downcomer annulus formed by the reactor vessel and the core barrel and up through the core and the coolant outlet plenum. It leaves the reactor vessel through the outlet nozzles.

There are, however, several bypass flow paths:

- Flow through the spray nozzles into the upper head for head cooling purposes.

This bypass flow is supplied by water from the downcomer annulus.

The fluid is then directed from the upper dome to the upper plenum.

In the "hot dome" configuration, which is the design option chosen, this flow rate is, in normal operation, directed downwards through some guide thimbles and upwards through others.

- Flow entering the RCCA guide thimbles to cool the control rods, the poison rods (if used), neutron sources, and instrumentation.
- Leakage flow from the vessel inlet nozzle directly to the vessel outlet nozzle through the gap between the vessel and the barrel.
- Flow between the heavy reflector and the core barrel, and inside the heavy reflector for the purpose of cooling these components and which is not considered available for core cooling.
- Flow in the gaps between the fuel assemblies at the core periphery and the adjacent heavy reflector.

The above contributions are shown in Sub-chapter 4.4 - Table 2 [Ref-1]. The maximum design value of the core bypass flow is equal to 5.5% of the total vessel flow.

Of the total allowance, 2.0% is associated with core bypass and the remainder with internals bypass (which correspond to bullets 1, 3, 4 and 5 of the above list). Calculations have been performed using tolerances specified in the drawings in the worse direction and accounting for uncertainties in pressure losses.

### 2.6.2. Core inlet flow maldistribution

The inlet flow distribution is generally non-uniform. Investigations with FLICA III-F involving decreasing the flow rate through a limited inlet area of the core indicate that there is a rapid redistribution up to one-third of the core height [Ref-1] and that consequently the inlet flow maldistribution has a negligible impact on the hot channel DNBR. This flow redistribution is due to the redistribution of fluid velocities. Consequently, the flow maldistribution at the core inlet induces no penalty on DNBR value or position and no penalty is included in assessing the DNBR.

### 2.6.3. Core vessel pressure drops

Unrecoverable pressure losses occur as a result of viscous drag (friction) and/or geometry changes (form losses) in the fluid flow path. The flow field is assumed to be incompressible, turbulent, single-phase water. These assumptions apply to the core and vessel pressure drop calculations for the purpose of establishing the Reactor Coolant System (RCS) loop flow rate. Two-phase considerations are neglected in the vessel pressure drop evaluation because the core average void is negligible.

Two phase flow considerations are however considered in the core thermal sub-channel analyses.

Core and vessel pressure losses are calculated by equations of the form:

$$\Delta P_L = \left( K + F \frac{L}{D_e} \right) \frac{\rho V^2}{2} \times 10^{-5}$$

where:

$\Delta P_L$  : Unrecoverable pressure drop, bar

$\rho$  : Fluid density, kg/m<sup>3</sup>

L : Length, m

$D_e$ : Equivalent diameter, m

V : Fluid velocity, m/s

K : Form loss coefficient, dimensionless

F : Friction loss coefficient, dimensionless.

Because of the complex core and vessel flow geometry, precise analytical values for the form and friction loss coefficients are not available. Consequently, experimental values for these coefficients are obtained from geometrically similar models.

The full power operation pressure drop values are shown in Sub-chapter 4.4 - Table 2 [Ref-1]. They are the irrecoverable pressure drops across the vessel, including the inlet and outlet nozzles, and across the core, including the fuel assembly, lower and upper core plates. These pressure drops are based on best estimate nominal plant operating conditions.

The core pressure drop characteristics are determined from hydraulic tests of 17 x 17 advanced fuel assemblies. These tests are carried out in a test loop under a wide range of Reynolds number, encompassing the range found in a PWR core.

The vessel pressure drops are obtained by combining the core loss with correlation of scale model hydraulic test data on a number of vessels, and from loss relationships.

Tests of the primary coolant loop flow rates will be made (see section 5.1) during the plant start-up tests to verify that the flow rates used in the design, which are determined in part from the pressure losses calculated by the method described here, are conservative.

#### **2.6.4. Hydraulic loads**

The highest hydraulic loads on vessel components are reached at maximum flow rate conditions.

At nominal operating conditions, the hydraulic loads are calculated from the mechanical flow rate, assuming the minimum core bypass flow rate value.

For cold shutdown conditions, the hydraulic loads are calculated with the same flow rates (vessel and core bypass), but with a different coolant density. This is the bounding case for normal operation.

Pump over-speed transient conditions, which could produce flow rates 20% greater than mechanical design flow rates, are used to determine the bounding hydraulic load in transient conditions.

Hydraulic tests have been used to check the value of hydraulic loads during pump over-speed transients at mechanical design flow under both hot and cold conditions.

#### **2.6.5. Internal hydraulic design**

The EPR Reactor Pressure Vessel (RPV) and RPV internals present some features that are new compared with previous designs and which are significant for the reactor's hydraulic design. These developments result from the design options chosen, new requirements, or from the merging of preceding French and German designs.

The most important developments are (see Sub-chapter 3.4):

Lower internals:

- The Flow Distribution Device, located below the core support plate, which ensures a relatively uniform flow rate distribution at core inlet and prevents vortices from forming inside the lower plenum. This new feature results from the EPR option of having no RPV bottom penetrations, which leaves the lower plenum empty.
- The Heavy Reflector, which is a massive component that replaces the baffle plates around the core cavity.

Upper internals:

- The design of the control rod guide thimble and normal support columns has been adapted to fit both the CRDM design (derived from the KONVOI design) and the EPR core and fuel assembly characteristics (driven by the French standards).

In addition, there are other developments in the RPV from the current designs, including an increase in core size, an increase in the number of radial keys (eight instead of six), and an increased radial gap in the downcomer annulus.

Because of those developments, it needs to be confirmed that the global RPV hydraulics meets the hydraulic performance requirements. This means the flow distribution at core inlet and outlet remains adequate so that sufficient mixing takes place upstream of the core inlet between the four loop flows, that the internals are adequately cooled, and that their mechanical design ensures safe operation.

This design is performed in three steps:

- First step: preliminary design

From operating experience feedback from other plants (French N4 and P4 and German KONVOI Nuclear Power Plants) or from experimental data.

- Second step: design checking and optimisation

By performing local Computational Fluid Dynamics (CFD) calculations, with the computer code STAR-CD, which is described in Appendix 4.

- Third step: design validation

By performing validation tests of the final design, comprising:

- Final validation tests before RPV manufacturing
- Commissioning tests before plant start-up.

## **2.7. THERMAL EFFECTS OF OPERATIONAL TRANSIENTS**

DNB core safety limits are generated as a function of coolant temperature, pressure, core power, and the axial and radial power distributions. Operation within these DNB safety limits ensures that the DNB design basis is met.

Section 4.1 gives a description of the low DNBR protection and the low DNBR trip threshold setting. This function provides adequate protection for both steady state operation and for anticipated operational transients that are slow with respect to fluid transport delays in the reactor coolant system. Additional specific protection is provided for fast transients and transients from hot zero power.

## **2.8. UNCERTAINTIES**

### **2.8.1. Critical heat flux**

#### **2.8.1.1. Treatment of uncertainties in DNBR calculations**

A statistical approach is used to combine uncertainties affecting the DNBR.

The random uncertainties whose probability distribution is known are statistically treated. The remainder are treated deterministically.

This approach is used to ensure that the DNBR criteria are met for all transients except for uncontrolled RCCA rod withdrawal from subcritical conditions or during start-up at low power, and for a steam line break transient, for which the uncertainties are combined deterministically.

**2.8.1.2. Overall DNBR uncertainty assessment**

**2.8.1.2.1. Statistical approach**

To relate the uncertainties affecting the DNBR to the variation in DNBR, a variable, defined by the following equation, is used:

$$Y = \frac{DNBR_r}{DNBR_c}$$

where  $DNBR_r$  is the actual DNBR value and  $DNBR_c$  is the calculated value determined by taking best estimate values for all the parameters involved.

$DNBR_c$  is the DNBR value calculated on-line by the algorithm implemented in the surveillance and protection system.

Thus, Prob ( $DNBR_r > T$ ) = 95% with a 95% confidence level is equivalent to: Prob ( $DNBR_c \times Y > T$ ) = 95% with a 95% confidence level.

If  $m$  and  $\sigma$  are the mean value and the standard deviation of the probability distribution for the random variable  $Y$ , the Prob ( $DNBR_c \times Y > T$ ) = 95% with a 95% confidence level is guaranteed provided  $DNBR_c > T / mY (1-1.645 V_Y)$ .

$DNBR_r$  is a random variable that can be decomposed as the product of the following random variables:

$$DNBR_r = \frac{\Phi_{rc}}{\Phi_{cp}} \times \frac{\Phi_{cp}}{\Phi_{IDC}} \times \frac{\Phi_{IDC}}{\Phi_{rl}} \times P$$

Where:

$\Phi_{rc}$  = actual critical heat flux,

$\Phi_{cp}$  = critical heat flux predicted by the CHF predictor,

$\Phi_{IDC}$  = local heat flux calculated by the Design Code,

$\Phi_{rl}$  = actual local heat flux at the same TH conditions,

$P$  = a penalty factor,

$\frac{\Phi_{cp}}{\Phi_{IDC}}$  =  $DNBR_{DC}$ , i.e. the DNBR value calculated by the design code.

$DNBR_{DC}$  is a random variable which is a function of the system random variables ( $T^\circ$ , P, Local Power, etc).

$DNBR_{DC}$  can be also decomposed as follows:

$$DNBR_{DC} = \frac{DNBR_{DC}}{DNBR_{DC0}} \times \frac{DNBR_{DC0}}{DNBR_{ao}} \times DNBR_{ao}$$

Where:

$DNBR_{DC0}$  =  $DNBR$  calculated by the design code at the best estimate values,

$DNBR_{ao}$  =  $DNBR$  calculated on-line by the I&C algorithm at the same best estimate values.

Consequently:

$$Y = \frac{DNBR_r}{DNBR_{ao}} \times \frac{\Phi_{rc}}{\Phi_{cp}} \times \frac{DNBR_{DC}}{DNBR_{DC0}} \times \frac{DNBR_{DC0}}{DNBR_{ao}} \times \frac{\Phi_{IDC}}{\Phi_{rl}} \times P$$

Y is the product of a factor P and of the following random variables:

- $\frac{\Phi_{rc}}{\Phi_{cp}}$ : The probability distribution of this variable is derived from the FC-CHF correlation. It is a normal distribution characterised by a mean value  $m_c$  and a standard deviation  $\sigma_c$ , as discussed in section 2.2.
- $\frac{DNBR_{DC}}{DNBR_{DC0}}$ : This random variable is a function of the following independent random variables:
  - Plant operating parameters (which are measured online):
    - Inlet temperature
    - Reactor pressure
    - Local power
    - Measured relative primary flow rate.
  - Parameters which cannot be measured but which influence the  $DNBR$ :
    - Pellet uncertainties related to enrichment/diameter/dishing ( $F_{\Delta H}^E, F_Q^E$ )

The probability distribution of this variable representative of overall system uncertainty is characterised by a mean value  $m_s$  and a standard deviation  $\sigma_s$ .

- $\frac{DNBR_{DC0}}{DNBR_{ao}}$  : This random variable represents the uncertainty in the I&C DNBR algorithm.

The probability distribution of this variable is characterised by the two parameters  $m_a$  and  $\sigma_a$ .

- $\frac{\Phi_{DC}}{\Phi_{fl}}$  : This random variable represents the uncertainty in the design code. Its probability distribution is characterised by the two parameters:  $m_{DC}$ ,  $\sigma_{DC}$ .
- An additional uncertainty representing the differences between the transient and steady state uncertainties must also be taken into account.

This uncertainty accounts for any discrepancy introduced by using local fluid properties from transient accident analysis to determine the DNBR under steady-state conditions. It is independent of the uncertainties discussed above.

The parameters characterising the probability distribution are  $m_{tss}$ ,  $\sigma_{tss}$ .

The factor P corresponds to all the uncertainties which will be treated deterministically, and include:

- Absolute total flow rate
- Core bypass flow
- Rod bow effect: RBP
- Neutronic data
- Actuation of the trip limit.

Except for the rod bow, all these uncertainties are directly taken into account within parameters used during transient analysis.

Sub-chapter 4.4 - Table 3 summarises all the variables.

As all the above mentioned variables (measured parameters, I&C algorithm, CHF predictor, design code, manufacturing tolerances) can be considered as independent and the perturbations from the mean value are small. The standard deviation  $V_Y$  accounting for the uncertainty distribution related to DNBR is calculated as:

$$V_Y^2 = \left(\frac{\sigma_Y}{m_Y}\right)^2 = \left(\frac{\sigma_c}{m_c}\right)^2 + \left(\frac{\sigma_s}{m_s}\right)^2 + \left(\frac{\sigma_a}{m_a}\right)^2 + \left(\frac{\sigma_{tss}}{m_{tss}}\right)^2 + \left(\frac{\sigma_{DC}}{m_{DC}}\right)^2 \quad (1)$$

The terms in Equation (1) are defined in section 2.8.2.

Moreover, the probability distribution function of Y has an approximately normal distribution with:

- The mean value:  $m_Y = m_c \times m_s \times m_a \times m_{tss} \times m_{DC} \times P$ ,
- The standard deviation  $\sigma_Y = m_Y \times V_Y$ .

Consequently, the probability that the DNBR will be greater than a threshold T is 95% with a 95% confidence level, provided DNBR is greater than the threshold  $DNB_{th}$  defined as:

$$DNB_{th} = \frac{T}{m_Y (1 - 1.645 V_Y)}$$

All the terms of this equation (1) are calculated separately except for  $\sigma_S/m_S$  which is derived using a Monte-Carlo method.

### 2.8.1.2.2. *Deterministic approach*

For some specific transient analysis, a deterministic approach is considered, where all the uncertainties mentioned above are treated deterministically.

Moreover, as the simplified on-line DNBR calculation is not used to protect the core against DNB for transients concerned by the deterministic approach, either by the protection system or by monitoring DNB against the Limiting Condition of Operation (LCO), each parameter which impacts DNBR must be monitored against a specific LCO and thus its uncertainty has to be accounted for.

These parameters are, for example:

- Average primary temperature
- Reactor pressure
- Local power.

With regard to the power distribution, the transient analysis assumes the most adverse one.

#### Design code and mixing coefficient uncertainty

The results of a sensitivity study with the design code show that the minimum DNBR in the hot channel is relatively insensitive to variations in the core-wide radial power distribution (for the same value of  $F_{\Delta H}^N$ ).

Studies have been performed to determine the sensitivity of the minimum DNBR in the hot channel to the radial and axial computational cell size, the inlet velocity, the pressure drop coefficient, the power distributions, the mixing coefficients, and the void model.

The results of these studies show that the minimum DNBR in the hot channel is relatively sensitive to variations in three of them: the mixing coefficients, the two-phase model, and the radial distribution of the grid pressure drop coefficients.

For the fuel grid, numerous mixing tests have been performed using the same experimental configurations as the one used for CHF tests.

These mixing tests have resulted in an average value of mixing coefficient significantly greater than the design value of 0.043 used in the design code calculations (see section 2.2.3).



### 2.8.2. Justification of statistical combination of uncertainties

As explained above a statistical approach is used to combine the following uncertainties affecting the DNBR:

- CHF predictor uncertainty ( $m_C, \sigma_C$ )
- Overall system uncertainty ( $m_S, \sigma_S$ )
- Algorithm uncertainty ( $m_a, \sigma_a$ )
- Design code uncertainty ( $m_{DC}, \sigma_{DC}$ )
- Transient versus steady-state uncertainty ( $m_{tSS}, \sigma_{tSS}$ ).

Random independent parameters for which the probability distribution is well known are treated statistically.

- CHF predictor uncertainty

Comparison of the FC-CHF correlation with CHF test results has provided the probability distribution of the ratio of measured-to-predicted CHF. The ratio is normally distributed (see section 2.2).

- Overall system uncertainty

Two main types of uncertainties are defined; each of these uncertainties can be split up into several uncertainties.

- Uncertainties in Physical parameters measured on-line:

The following plant operating parameters are used for calculating the DNBR: the inlet temperature, the pressuriser pressure, the relative measured primary flow rate and the local power. The inlet temperature is derived from the cold leg temperature sensors; the pressuriser pressure is derived from the primary pressure sensors; the relative measured primary flow rate is derived from the Reactor Coolant Pump speed sensors and the power density distribution of the hot channel is directly derived from the nuclear in-core instrumentation by Self Powered Neutron Detectors (SPND). Each measurement is independent of the others (Temperature sensor on the cold leg, pressure sensor on the top of pressuriser, speed sensor on the reactor coolant pump and in-core for SPND). For example, there is no relationship between the temperature sensor uncertainty due to calibration error and the equivalent uncertainties in pressuriser pressure sensor or reactor coolant pump speed.

Several devices are used to derive the signal to the protection system from that provided by the sensor (e.g. for temperature: ohm-ampere converter, ampere-volt converter, isolation module if required, and analogue/numerical converter). Each of these devices has a random and independent uncertainty that is treated statistically.

The power density distribution of the hot channel introduces the following uncertainties: the Aeroball Measuring System accuracy (taking into account the activation rate accuracy, the relative power density reconstruction, the burnup interval length, and the number of instrumented assemblies), and the SPND signal accuracy (drift, allowance for burnable absorbers, etc).

The global uncertainty can be divided into several independent probability distributions (sensor, transmitter calibration, etc.) and uncertainties. The resultant cumulative probability distribution of such a high number of random variables is a normal distribution as is generally the case for measurement uncertainties.

- Pellet manufacturing allowance uncertainties:

The factor  $F_{\Delta H}^E$  accounts for variations in those fabrication variables which affect the heat generation rate along the flow channel. These variables are pellet diameter, density and U-235 enrichment. Uncertainties in these variables are determined from sampling of manufacturing data. The resulting uncertainty is independent of the uncertainties discussed above. The distribution is normal.

- Algorithm uncertainty

This uncertainty accounts for the difference between the design code calculation and the on-line DNBR algorithm calculation at the same thermal and hydraulic conditions. The algorithm is fitted to the results of design code calculations.

The probability distribution of the difference between the on-line DNBR algorithm and the design code is derived by statistical analysis. The distribution is normal.

- Design code uncertainty

The design code uncertainty includes all the effects of analysing the complete core with a numerical code. Since the design code is used for the analysis of the heat flux tests, the predicted heat fluxes for each set of experimental data include the design code uncertainty and consequently also the parameters  $m$  and  $\sigma$  in the predictive model.

- Transient versus steady-state uncertainty

This uncertainty accounts for any discrepancy introduced by the calculation of DNBR under steady-state conditions using local fluid properties from transient analyses. It is independent of the uncertainties noted above. It is assumed to have a normal distribution.

### 2.8.3. Fuel and cladding temperatures

The fuel temperature is a function of oxide, cladding, gap, and pellet conductance. Uncertainties in the fuel temperature calculation are essentially of two types:

- Fabrication uncertainties, such as variations in the pellet and cladding dimensions,
- The pellet density and modelling uncertainties such as variations in the pellet conductivity and the gap conductance.

These uncertainties have been quantified by comparing the thermal model with the in-core thermocouple measurements, by out-of-core measurements of the fuel and cladding properties, and by measurements of the fuel and cladding dimensions during fabrication. The resulting uncertainties are then used in all calculations of the fuel temperature.

In addition to the temperature uncertainty described above, the measurement uncertainty in determining the local power and the effect of density and enrichment variations on the local power are considered in deriving the heat flux hot channel factor. These uncertainties are described in Sub-chapter 4.3.

There is an uncertainty in the cladding temperature associated with the uncertainty in the oxide thickness. Because of the excellent heat transfer between the surface of the rod and the coolant, the film temperature drop does not appreciably contribute to the uncertainty in cladding temperature.

#### **2.8.4. Hydraulic**

- Uncertainties in pressure drops

Core and vessel pressure drops are based on the best estimate flow. The uncertainties in these parameters are based on the uncertainties in both the test results and in the analytical derivation of the equivalent reactor values.

The core and vessel pressure drops are principally used to determine the reactor coolant system flow rates. In addition, tests on the reactor coolant pump prior to initial criticality will be made to confirm that a conservative reactor coolant pump coolant flow rate has been used in the design and analyses of the plant.

- Uncertainties due to inlet flow maldistribution

The effects of uncertainties in the inlet flow maldistribution criteria used in the core thermal analyses are discussed in section 2.6.2.

- Uncertainties in flow rates

The thermal-hydraulic design flow rate, which is defined for use in core thermal performance assessments, accounts for both prediction and measurement uncertainties.

In addition, a maximum of 5.5% of the thermal-hydraulic design flow rate is assumed to be ineffective for core heat removal capability because it bypasses the core through the various available vessel flow paths described in section 2.6.1.

- Uncertainties in hydraulic loads

As discussed in section 2.6.4, the bounding hydraulic loads on the fuel assembly are evaluated in normal operation for cold shutdown conditions and in transient conditions for a pump over-speed transient, which gives flow rates 20% greater than the mechanical design flow rate. The mechanical design flow rate is 8% greater than the best estimate or most likely flow rate value for the actual plant operating condition.

- Uncertainties in internal hydraulic design

Uncertainties are taken into account either by assuming conservative boundary conditions for the calculations, or through conservatism inherent in the code, or in the numerical schemes used to perform the calculation.

### **3. OPERATING THERMAL AND HYDRAULIC REACTOR PARAMETERS**

#### **3.1. TEMPERATURE POWER OPERATING MAP**

The relationship between the reactor coolant system temperature and the power [Ref-1] are shown in Sub-chapter 4.4 - Figure 4 for thermal-hydraulic design, best estimate and mechanical design flow rates.

#### **3.2. THERMAL AND HYDRAULIC CHARACTERISTICS**

The thermal and hydraulic characteristics are given in Sub-chapter 4.4 - Table 1.

### **4. ANALYSIS METHODS AND DESIGN DATA**

#### **4.1. METHODOLOGY USED FOR TRANSIENT ANALYSIS**

Low DNBR Reactor Trip (RT) and Limiting Conditions of Operation (LCO) settings are considered.

The transients to be analysed are events of PCC-2 and also some specific transient events of PCC-3 or PCC-4 (e.g. steam line break).

The methodology depends on whether or not the reactor is tripped on low DNBR.

For tripping on low DNBR channel, the objective is to derive the required trip setting. For tripping on other parameters the objective is to define, for each transient, the required DNBR limit.

Transients are split up into three categories:

- Type I transients: transients from power for which the low DNBR protection is effective.
- Type II transients: transients from power for which the low DNBR protection is not effective.
- Type III transients: transients from hot zero power (uncontrolled RCCA bank withdrawal from a subcritical or low-power start-up and steam line break (SLB)).

##### **4.1.1. Transients from power (low DNBR reactor trip and LCO setting)**

As the low DNBR protection channel or the low DNBR surveillance channel is based directly on the simplified DNBR variable derived by the algorithm, the low DNBR trip threshold and the low DNBR LCO threshold are set taking into account the reconstruction uncertainties in the derived value and the measurement accuracy.

DNB is avoided by keeping the on-line calculated values of DNBR greater than the limits.

The uncertainties can be different for the two systems, as they are related to system accuracy and system operational conditions.

For the reactor trip and the operating limit setting, it is necessary to split transients in two classes:

- The transients for which the low DNBR reactor trip is effective (type I transients):

These are characterised by the following conditions:

- Parameters that influence DNBR during the transient are taken into account in the low DNBR protection channel,
- The rate of change of influential parameters is not too fast to be detected by the low DNBR protection channel.

The low DNBR I&C channel trip is actuated whenever DNBR reaches the Safety Criterion (SC).

The variable  $Y = \frac{DNBR_r}{DNBR_{PS}}$  is characterised by a mean value ( $m_Y^{PS}$ ) and a standard deviation ( $\sigma_Y^{PS}$ ).

$DNBR_{PS}$  is the DNBR value calculated by the protection system algorithm.

The low DNBR I&C channel trip is then actuated when the DNBR value calculated by the protection system is lower than the threshold value  $DNBR_{PS}$  calculated from

$$DNBR_{PS} = \frac{SC}{m_Y^{PS} (1 - 1.645 \sigma_Y^{PS})}$$

This means that the probability of avoiding DNB is 95% at 95% confidence level.

- The transients for which the low DNBR protection is not effective (type II transients):

In this case reactor trip is achieved using only specific parameters (in many cases only one, e.g. low pump speed). It is therefore necessary to assume initial values for other parameters not taken into account in the RT channel, and hence to define the values to be observed by the LCO surveillance system.

The most critical assumption is linked to the power distribution and the best way to meet this is to monitor the initial DNBR value.

During normal operation, the on-line calculated DNBR value must be kept above a low DNBR limit (LCO), such that DNB is avoided in the course of the anticipated transient.

The most typical transient of this kind is the complete loss of forced reactor coolant flow.

To define the LCO I&C channel DNB settings for these transients, the maximum DNBR variation is calculated for all transients of this category.

The transient leading to the largest DNBR variation determines the low DNBR LCO limit:

$$\text{DNB}_{\text{LCO}} = \frac{[\text{SC} + (\Delta\text{DNBR})_{\text{max}}]}{m_Y^{\text{SS}} (1 - 1.645 V_Y^{\text{SS}})}$$

Where  $m_Y^{\text{SS}}$  and  $V_Y^{\text{SS}}$  are the mean value and the standard deviation of the variable

$$Y = \frac{\text{DNBR}_r}{\text{DNBR}_{\text{SS}}} \text{ and } \text{DNBR}_{\text{SS}} \text{ is the DNBR value calculated by the surveillance system.}$$

During normal operation, the DNBR must always remain above the low DNBR LCO limit, to ensure that the DNB criterion will be met if this type of transient occurs.

#### 4.1.2. Transients from hot zero power (DNBR design limit)

These transients, named Type III transients, are:

- Uncontrolled RCCA rod withdrawal from a subcritical or low power start-up
- Main and minor steam system piping failure (steam line break).

Specific analysis is performed for them. Specific protection is necessary because the low DNBR I&C channel is ineffective.

The minimum DNBR is calculated through the transient and must always be greater than the DNBR design limit assessed deterministically.

This limit only includes:

- The correlation/design code uncertainty
- The rod bow uncertainty except for Steam Line Break (SLB), since no rod bow effect exists at low pressures.

Consequently:

- For high pressures (above 120 bar - e.g. uncontrolled RCCA rod withdrawal from a subcritical or low power start-up), the DNBR design limit, assuming the most conservative value of RBP (0.068), is 1.21.
- For low pressures (under 120 bar - e.g. SLB): the DNBR design limit = 1.12

## 4.2. INFLUENCE OF POWER DISTRIBUTION

The core power distribution, which is largely established at beginning-of-life by the fuel enrichment, loading pattern, and the core power level are also a function of variables such as control rod worth and position, and fuel depletion throughout lifetime. The core radial enthalpy rise distributions, as determined by the integral of power of each channel, are of greater importance for DNB analyses. These power distributions are characterised by  $F_{\Delta H}^N$  and axial heat flux profiles.

Given the local power density  $q'(W/cm)$  at a point  $x, y, z$  in a core with  $N$  fuel rods and height  $H$ , the nuclear enthalpy rise hot channel factor is given by:

$$F_{\Delta H}^N = \frac{\text{hot rod power}}{\text{average rod power}} = \frac{\max \int_0^H q'(x_o, y_o, z) dz}{\frac{1}{N_{\text{allrods}}} \sum \int_0^H q'(x, y, z) dz}$$

Where  $x_o, y_o$  are the position coordinates of the hot rod.

The way in which  $F_{\Delta H}^N$  is used in the DNBR calculations is important.

The location of minimum DNBR depends on the axial profile, and the value of DNBR depends on the enthalpy rise to that point. Basically, the maximum value of the rod power integral is used to identify the most likely rod for minimum DNBR. An axial power profile is obtained which, when normalised to the value of  $F_{\Delta H}^N$ , recreates the axial heat flux along the limiting rod. The surrounding rods are assumed to have the same axial profile with rod average power, which are typical distributions found in hot assemblies. In this manner, worst case axial profiles can be combined with worst case radial distributions for reference DNB calculations.

It should be noted again that  $F_{\Delta H}^N$  is an integral and is used as such in DNB calculations. Local heat fluxes are obtained by using hot rod and adjacent rod explicit power shapes which take into account variations in horizontal power shapes throughout the core.

The enthalpy rise hot channel factor  $F_{\Delta H}$  corresponds to:

$$F_{\Delta H} = \max_{xy} (P_{\Delta H}(x, y))$$

Where  $P_{\Delta H}(x, y)$  is the radial enthalpy rise distribution of the channel  $(x, y)$ :

$$P_{\Delta H}(x, y) = \frac{\int_0^H P(x, y, z) dz}{\int_0^H dz}$$

And  $P(x, y, z)$  is the relative power in the channel  $(x, y)$  at the height  $z$ .

The average relative power of each channel is the mean of relative power of all rods surrounding the channel weighted by the fraction of their heating perimeter located in the channel.

The design studies are performed with power distributions calculated by the neutronic design codes.

For Type I and Type II transients (see section 4.1) the core-related I&C protection functions protect the core against extreme power distributions.

The power density distribution of the hot channel is directly derived from the nuclear in-core instrumentation by Self Powered Neutron Detectors (SPNDs).

Consequently the following two uncertainties are associated with the power density distributions:

- The reconstruction uncertainty
- The measurement accuracy.

For type III transients (see section 4.1) the uncertainty in the power distribution derives from the uncertainty in its calculation, which affects the DNBR value calculated by the design code.

For loss of coolant analyses (LOCA) a decoupling design value of  $F_{\Delta H}^N$  equal to 1.80 is used.

This takes into account the uncertainties in the power distribution calculations, the xenon penalty for azimuthal and radial oscillations, and a provision to cover different fuel loading patterns.

### **4.3. CORE ANALYSIS TOOLS**

The objective of the reactor core thermal design is to determine the maximum heat removal capability in all flow sub-channels and show that the core safety limits are not exceeded taking into account uncertainties due to both engineering and nuclear effects. The thermal design considers local variations in dimensions, power generation, flow redistribution, and mixing.

The design uses the FLICA III-F computer code (described in, Appendix 4) which has realistic matrix models that have been developed to account for hydraulic and nuclear effects on the enthalpy rise in the core. The behaviour of the hot assembly is determined by superimposing the power distribution between assemblies on the inlet flow distribution while allowing flow mixing and redistribution between assemblies. The average flow and enthalpy in the hottest assembly is obtained from the core-wide, assembly-by-assembly analysis. The local variation of power, fuel rod and pellet fabrication, and mixing within the hottest assembly are then superimposed on the average conditions of the hottest assembly in order to determine the conditions in the hot channel.

The transient and steady state FLICA III-F computer program has been used to determine coolant density, mass velocity, enthalpy, void fraction, static pressure, and DNBR distributions along parallel flow channels within a reactor core under all expected operating conditions.

### **4.4. THERMAL RESPONSE OF THE CORE**

The general thermal-hydraulic characteristics of the core during steady-state operating conditions are shown in Sub-chapter 4.4 - Table 1.

### **4.5. HYDRAULICS DATA**

Refer to Sub-chapter 4.4 - Tables 1 and 2 for the following:

- Bypass flow rates
- Pressure drops



- Best estimate flow values.

#### **4.6. HYDRODYNAMIC INSTABILITY**

The EPR pump head curve has a negative slope ( $\partial P/\partial G$  external  $< 0$ ), whereas the reactor coolant system pressure drop versus flow curve has a positive slope ( $\partial P/\partial G$  internal  $> 0$ ) over the PCC-1 and PCC-2 operational ranges. The criterion for stability is therefore met and thus Ledinegg instability will not occur.

The application of the Ishii method to reactors indicates that a large margin to density wave instability exists, e.g. increases of the order of 200% of rated reactor power would be required for the predicted inception of this type of instability.

The application of the Ishii method to the EPR plant is conservative due to the parallel open channel nature of PWR cores. For such cores, there is little resistance to the lateral flow leaving the flow channels with a high power density. There is also energy transfer from high power density channels to lower power density channels. This coupling with cooler channels has led to the judgment that an open channel configuration is more stable than a closed channel system considered in the analysis, for the same boundary conditions.

Additional evidence that flow instabilities do not adversely affect the thermal margin is provided by data from the rod bundle DNB tests. Many rod bundles have been tested over a wide range of operating conditions with no evidence of premature DNB or of inconsistent data which might be indicative of flow instabilities in the rod bundles.

In summary, it is concluded that thermal hydrodynamic instabilities will not occur in PCC-1 and PCC-2 modes of reactor operation. A large power margin to the inception of such instabilities is predicted (greater than twice the rated power).

### **5. TESTING AND VERIFICATION**

#### **5.1. TESTS PRIOR TO INITIAL CRITICALITY**

Reactor coolant flow tests are performed following fuel loading and at several power levels after the plant start-up. The results of the successive enthalpy balances performed enable determination of the coolant flow rates at reactor operating conditions. These tests confirm that the correct coolant flow rates have been used in the core thermal and hydraulic analysis.

#### **5.2. INITIAL POWER AND PLANT OPERATION**

Core power distribution measurements are made at several core power levels. These tests are used to ensure that the values of the parameters used in the evaluation of the power distribution and the enthalpy rise factor are correct.

### 5.3. COMPONENT AND FUEL INSPECTIONS

Inspections are performed on the manufactured fuel. Fabrication measurements critical to thermal and hydraulic analyses are obtained to verify that the engineering hot channel factors used in the design analyses are met.

## 6. INSTRUMENTATION REQUIREMENTS

### 6.1. LOW DNBR FUNCTIONS

There are two low DNBR I&C functions:

- The low DNBR protection function, which actuates the Reactor Trip (RT)
- The low DNBR Limiting Conditions of Operation (LCO) function (surveillance function).

The use of DNBR on-line calculations in the protection and surveillance systems enables the DNBR criterion to be met by defining a low DNBR reactor trip channel and a low DNBR LCO channel based directly on the reconstructed variable representative of the phenomenon to be avoided.

The low DNBR protection function actuates a reactor trip which protects the fuel against DNB during accidental transients, whatever the Postulated Initiating Event (PIE) leading to an uncontrolled decrease of the DNBR. The low DNBR LCO function ensures a sufficient margin to the DNBR criterion during normal operation in order to accommodate PIEs leading to a significant decrease in DNBR. During PCC-1 events, the DNBR value must be kept above the  $DNBR_{LCO}$  limit such that, should a PIE occur for which the low DNBR protection is not effective, DNB is avoided (see section 4.1).

Exceeding this LCO initiates the following countermeasures:

- On the first setting, an alarm, freezing of both RCCA withdrawal and the load increase
- On the second setting, a reactor power reduction by the insertion of rod banks and, if necessary, an appropriate turbine load reduction.

Both I&C DNBR algorithms for protection and surveillance are based on the same principles.

The calculation of the minimum DNBR uses the following parameters:

- Power density distribution of the hot channel.
  - This is directly derived from the neutronic in-core instrumentation (SPND), which is described in Sub-chapter 7.6. The signals from the in-core detectors calibrated in power density units provide both local power and integrated power along the hot channel using a polynomial fit.
- Inlet temperature:
  - Derived from the cold leg temperature sensors.

- Pressure:
  - Derived from the primary pressure sensors
- Core flow rate:
  - Derived from the RCP [RCS] pump speed sensors.

The CHF is calculated using the FC-CHF correlation, described in section 2.2.1, using local thermal-hydraulic parameters, i.e. pressure, quality, and mass flow.

These parameters are calculated by a simplified single-channel model representing the hot channel without considering exchanges with neighbouring channels.

It is therefore part of the thermal-hydraulic design code to account for mass and energy exchanges between channels.

## 6.2. HIGH LINEAR POWER DENSITY (HLPD) FUNCTIONS

There are two high linear power density functions:

- The HLPD protection function
- The HLPD LCO function (surveillance function)

The safety criteria for melting at the centre of the fuel pellet are satisfied by meeting the decoupling criteria on the linear power density at the hot spot, which must remain lower than a certain limit.

Thus, the protection and surveillance systems enable the safety criteria for melting at the centre of the fuel pellet to be met by defining an HLPD reactor trip channel and a HLPD LCO channel directly based on the reconstruction of the linear power density at the hot spot.

The HLPD protection function actuates a reactor trip which protects the fuel against melting at the centre of the fuel pellet during accident transients, whatever the PIE leading to an uncontrolled increase of the linear power density.

The HLPD LCO function mainly ensures compliance with the core integrity criterion in case of Loss Of Coolant Accident (LOCA) or PIEs such as "RCP [RCS] pump shaft break" and/or "rod ejection".

Exceeding this LCO initiates the following countermeasures:

- On the first setting, an alarm, inhibiting RCCA withdrawal or RCCA insertion, depending on the axial power shape, and inhibiting load increase
- On the second setting, a reactor power reduction by the insertion of rod banks and, if necessary, an appropriate turbine load reduction.

A distortion of the power shape can be a cause, among others, for this limiting value to be reached. The limiting value depends on the core axial location (lower for the upper core half than for the lower core half) which means that this surveillance function also limits the axial power shape.

The calculation of the maximum linear power density value (W/cm) is derived directly from neutronic in-core measurements via the Self Power Neutron Detectors (SPNDs).

### 6.3. FIXED IN-CORE NEUTRONIC INSTRUMENTATION

The fixed in-core nuclear instrumentation system contains Self Powered Neutron Detectors (SPNDs), which are used to measure the local power density generated by the fuel elements (see Sub-chapter 7.6).

The detector fingers are located where they can give the maximum information on power density variations and their impact on the key core parameters ( $F_Q$ ,  $F_{\Delta H}$ ), especially under perturbed conditions.

The SPNDs are distributed homogeneously radially within the core so that their signals are representative of the key core parameters for different perturbation modes and fuel management regimes.

Twelve fuel assemblies are instrumented. Consequently the core is divided into 12 radial zones and each zone is monitored by one SPND finger.

The SPND fingers are distributed such that practically the whole core area is covered.

The location of instrumented assemblies and the different zones are shown in Sub-chapter 4.4 - Figure 5.

Each of the 12 SPND fingers contains six detectors.

In each finger, three SPNDs are located in the upper half of the core and the other three in the bottom half to detect the peak power density occurring in the upper and lower halves. This covers all possible power distributions (normal and accidental). Optimal axial positions are determined from the analysis of axial power shapes in transient conditions (see Chapter 14).

Axial locations are always between two grids to avoid flux depression in the vicinity of the grids.

For each finger, a region of the core volume called a "surveillance zone" is assigned. The fingers are calibrated against the Aeroball Measuring System (AMS) (see section 6.4) to reproduce:

- The peak power density
- The power distribution of the channel containing the maximum power density (AMS distribution), used for the on-line minimum DNBR calculation.

### 6.4. AEROBALL MEASURING SYSTEM (AMS)

The basic function of this movable in-core neutronic instrumentation system is to measure the neutron flux at different spatial points of the core (see Sub-chapter 7.6). The preliminary aeroball probe location is shown in Sub-chapter 4.4 - Figure 6. The flux map is used to get the axial neutronic power distribution of the hot channel of each fuel assembly (3-D image of the distribution).

From axial distributions, the following core parameters are deduced:

- The axial neutronic power of the hot channel of each fuel assembly and the and maximum core value of the parameter  $F_Q$
- The average axial neutronic core power distribution
- The integrated power along each assembly and hot channel enabling the derivation of the rise in enthalpy level in each assembly, and hence the maximum core value of the parameter  $F_{\Delta H}$ . The min DNB ratio is then calculated from the operating thermal-hydraulic conditions
- Quadrant power tilt ratio.

Core measurements can be used for the following:

- Verification of the correctness of core-build at first start-up and following reloads
- Calibration of fixed in-core and ex-core neutronic instrumentation
- Justification of the measurement uncertainties taken into account in monitoring systems
- Following fuel assembly burnup
- Investigation and diagnosis when operating in special or abnormal conditions.

The Aeroball Measuring System enables:

- Flux maps to be taken of all the different regions of the core, suitably weighting the effects of different fuel enrichments, the local effects of control rods, and radial variations. Claiming symmetry, nearly all assemblies, except those located at RCCA positions are instrumented.
- Measurements to be made which are distributed uniformly over the active height of the fuel assembly.

## **6.5. EXCORE NEUTRONIC INSTRUMENTATION**

The output of the three ranges of detectors (source, intermediate, and power) (see Sub-chapter 7.6), with the nucleonics, is used to limit the maximum power output of the reactor within their respective ranges.

The following neutron flux detectors are installed around the reactor in the primary shield:

- Three chambers for the source range installed at the core edge.
- Four chambers for the intermediate range installed at the core edge and positioned at mid-core height.
- Four detectors for the power range placed as near as possible to the reactor vessel. Each detector is axially dived into two sections and covers the whole active core height.

The three ranges of detectors are used as inputs to monitor neutron flux from shutdown to 120% of core power, with the capability of recording higher overpower excursions.

The output of the power range channels may be used for:

- Protecting the core against uncontrolled positive reactivity insertion. It is used mainly to provide protection against PIEs of PCC-3 (e.g. single RCCA withdrawal at power) or PCC-4 (e.g. RCCA ejection).
- Alerting the operator to an excessive power imbalance between the quadrants.
- Inhibiting RCCA bank movement.

**SUB-CHAPTER 4.4 - TABLE 1 (1/2)**

**Thermal-hydraulic Design Data**

Total core heat output (MWth)	4500
Number of loops	4
Nominal system pressure (absolute) (MPa)	15.5
Coolant flow:	
Core flow area (m <sup>2</sup> )	5.9
Core average coolant velocity (m/s)	5
Core average mass flow rate (g/cm <sup>2</sup> /s)	356
Total mass flow rate (kg/s)	22235 [Ref-1]
Core mass flow rate (t/h)	75643
Thermal design flow/loop (m <sup>3</sup> /h)	27185 [Ref-1]
Best estimate flow/loop (m <sup>3</sup> /h)	28320 [Ref-1]
Mechanical design flow /loop (m <sup>3</sup> /h)	30585 [Ref-1]
Coolant temperature (°C):	
Nominal inlet	295.6 [Ref-1]
Average rise in vessel	34.2 [Ref-1]
Average rise in core	36.0 [Ref-1]
Average in core	313.6 [Ref-1]
Average in vessel	312.7 [Ref-1]
Heat transfer:	
Heat transfer surface area (m <sup>2</sup> )	7960 [Ref-1]
Average core heat flux (W/cm <sup>2</sup> )	54.7
Maximum core heat flux (nominal operation) (W/cm <sup>2</sup> )	157.3
Average linear power density (with a cold geometry) (W/cm)	163.4
Peak linear power for normal operating conditions (W/cm)	470
Peak linear power protection setpoint (W/cm)	590

**SUB-CHAPTER 4.4 - TABLE 1 (2/2)**

**Thermal-hydraulic Design Data**

DNB ratio (for illustration):  Minimum DNBR under nominal operating conditions with: $F\Delta H = 1.61 - \cos 1.45$	2.6
Fuel assembly:  Number of fuel assemblies Fuel assembly pitch (cm) Active fuel height (cm) Lattice pitch (cm) Number of fuel rods per assembly Number of control rod assembly guide thimbles per assembly Outside fuel rod diameter (cm) Guide thimble diameter (cm)	241 21.504 420 1.26 265 24 0.95 1.245
Core power characteristics:  Power density in hot conditions (kW/core/10 <sup>-3</sup> m <sup>3</sup> )	94.6



**SUB-CHAPTER 4.4 - TABLE 2**

**Core Bypass Flow and Vessel and Core Pressure Losses**

I: Core bypass flow [Ref-2]	DESIGN VALUE (% of total vessel flow)
Head cooling flow	0.5
Control rod cluster guide thimble cooling flow	2.0
Leakage to outlet nozzles	1.0
Flow through the heavy reflector	1.5
Flow between the heavy reflector and the core	0.5
<b>Total core bypass flow</b>	<b>5.5</b>

II: Vessel and core pressure losses [Ref-1]	HEAD LOSS (bar)
Reactor vessel	3.44
Core	1.88

**SUB-CHAPTER 4.4 - TABLE 3**

**DNBR Uncertainties**

VARIABLE		Distribution	Standard Deviation	Mean Value
CHF predictor	$\Phi_{rd}/\Phi_{cp}$	Normal	$\sigma_c$	$m_c$
<u>System parameters</u> <sup>1</sup> :	$\frac{DNBR_{DC}}{DNBR_{DC0}}$	Normal	$\sigma_S$	$m_S$
- Inlet T°			$\sigma_T$	$m_T$
- Reactor pressure			$\sigma_p$	$m_p$
- Local power			$\sigma_{lp}$	$m_{lp}$
- Measured relative primary flow			$\sigma_Q$	$m_Q$
- $F_{\Delta H}^E$			$\sigma F_{\Delta H}^E$	$m F_{\Delta H}^E$
- $F_Q^E$			$\sigma F_Q^E$	$m F_Q^E$
I&C algorithm			$\frac{DNBR_{DCD}}{DNBR_{a0}}$	Normal
Transient versus steady state	$\Phi_{IDC}/\Phi_{rl}$	Normal	$\sigma_{tss}$	$m_{tss}$
Design code		Normal	$\sigma_{DC}$	$M_{DC}$
<u>Penalties</u> :	P	Constant	0	P
- Rod bow				RBP
- Absolute total flow				Thermal hydraulic
- Core bypass flow				Thermal hydraulic

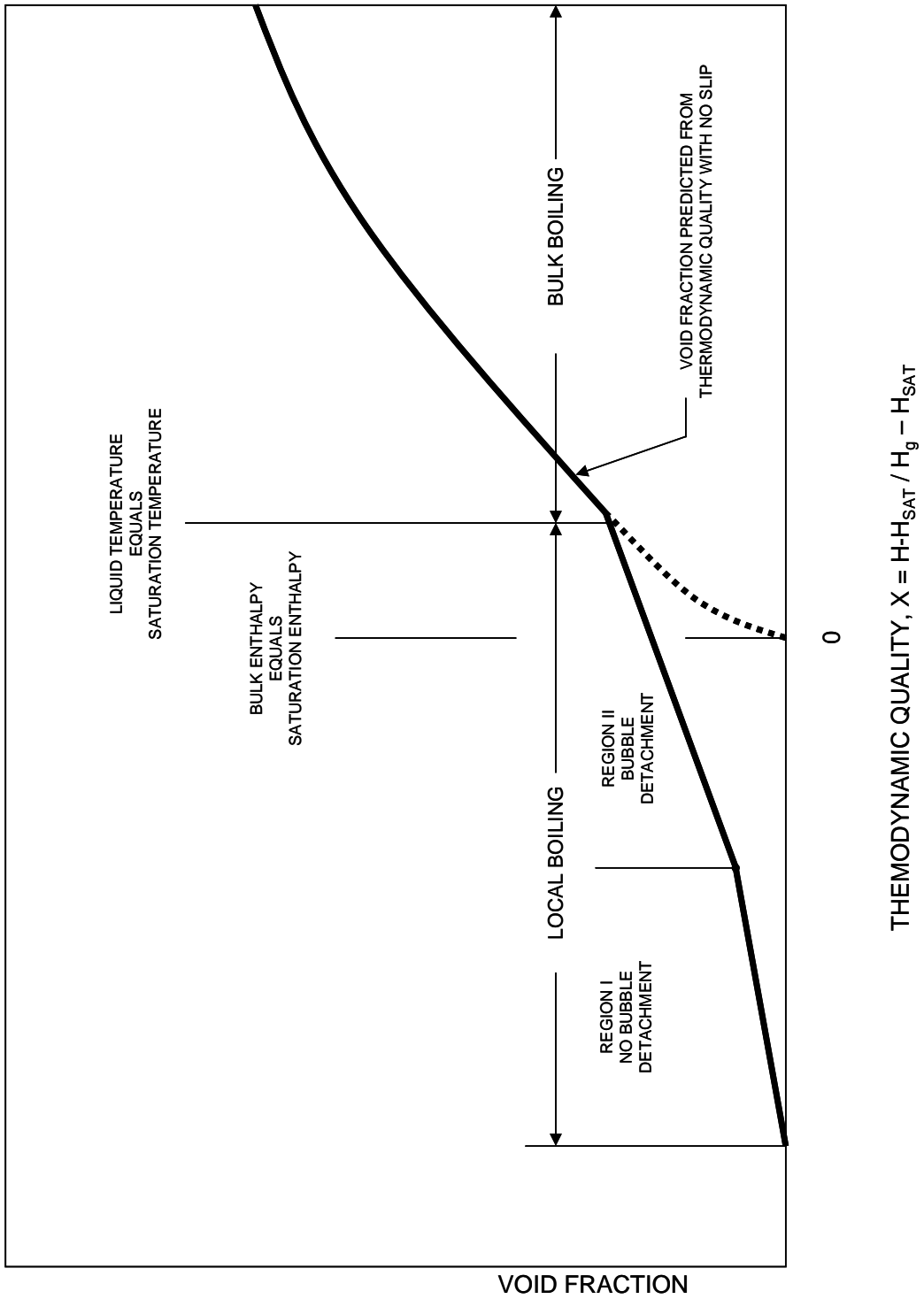
<sup>1</sup> For these parameters, if there is no systematic error, the mean value is equal to 1

{CCI Removed}

{CCI Removed}

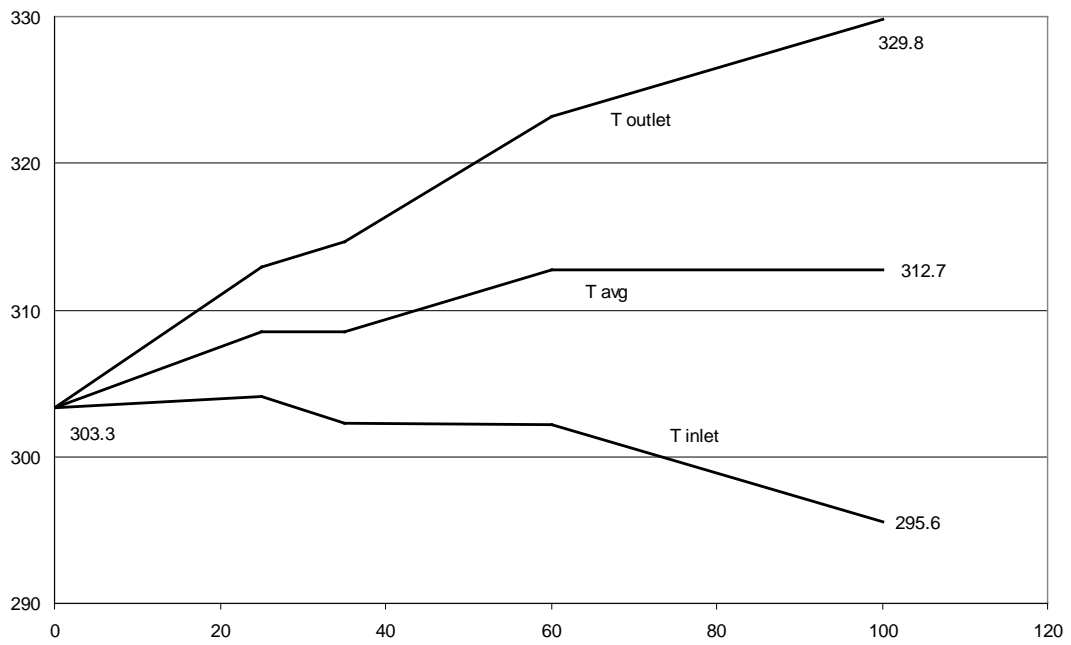
**SUB-CHAPTER 4.4 - FIGURE 3**

**Void Fraction versus Thermodynamic Quality**



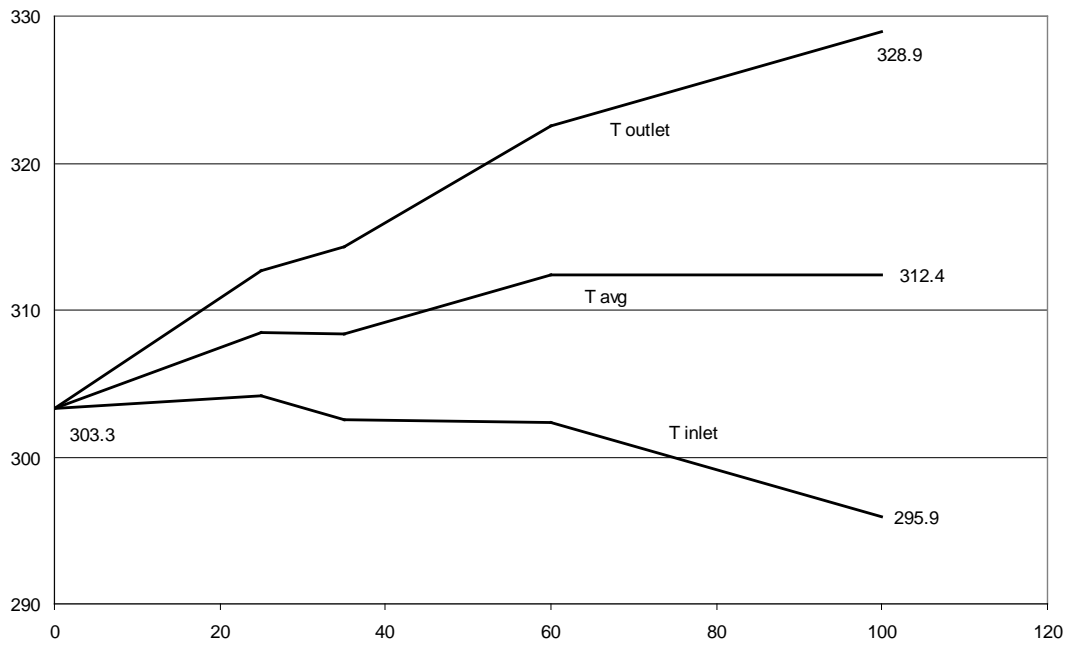
**SUB-CHAPTER 4.4 - FIGURE 4 (1/3)**

**Part Load Diagram at Thermal-Hydraulic Design Flow Rate**



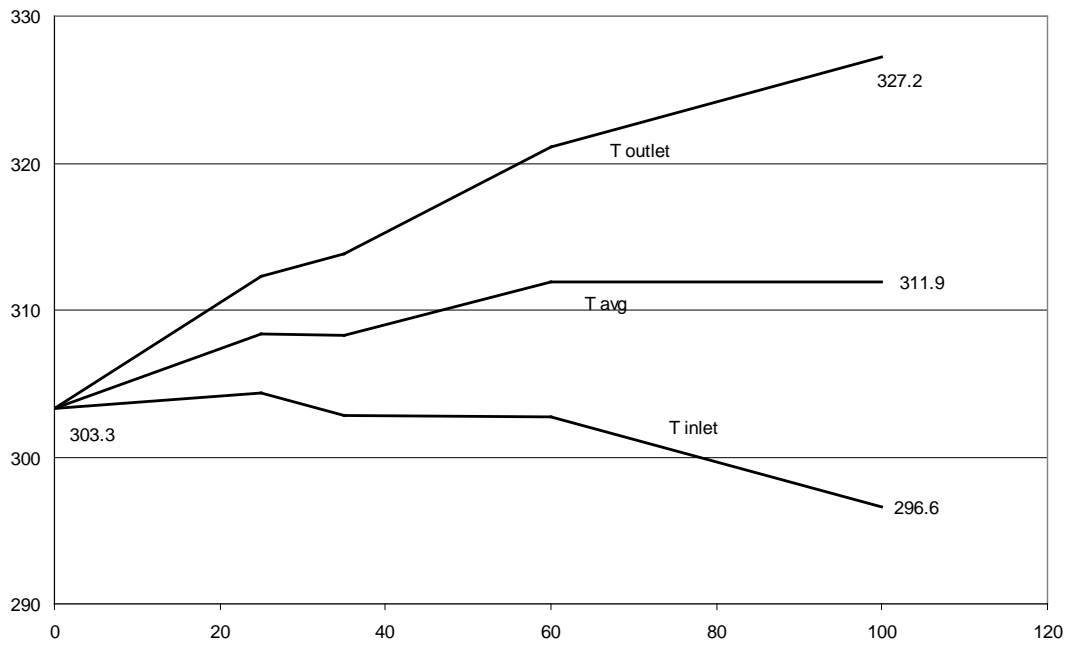
**SUB-CHAPTER 4.4 - FIGURE 4 (2/3)**

**Part Load Diagram at Best Estimate Flow Rate**



**SUB-CHAPTER 4.4 - FIGURE 4 (3/3)**

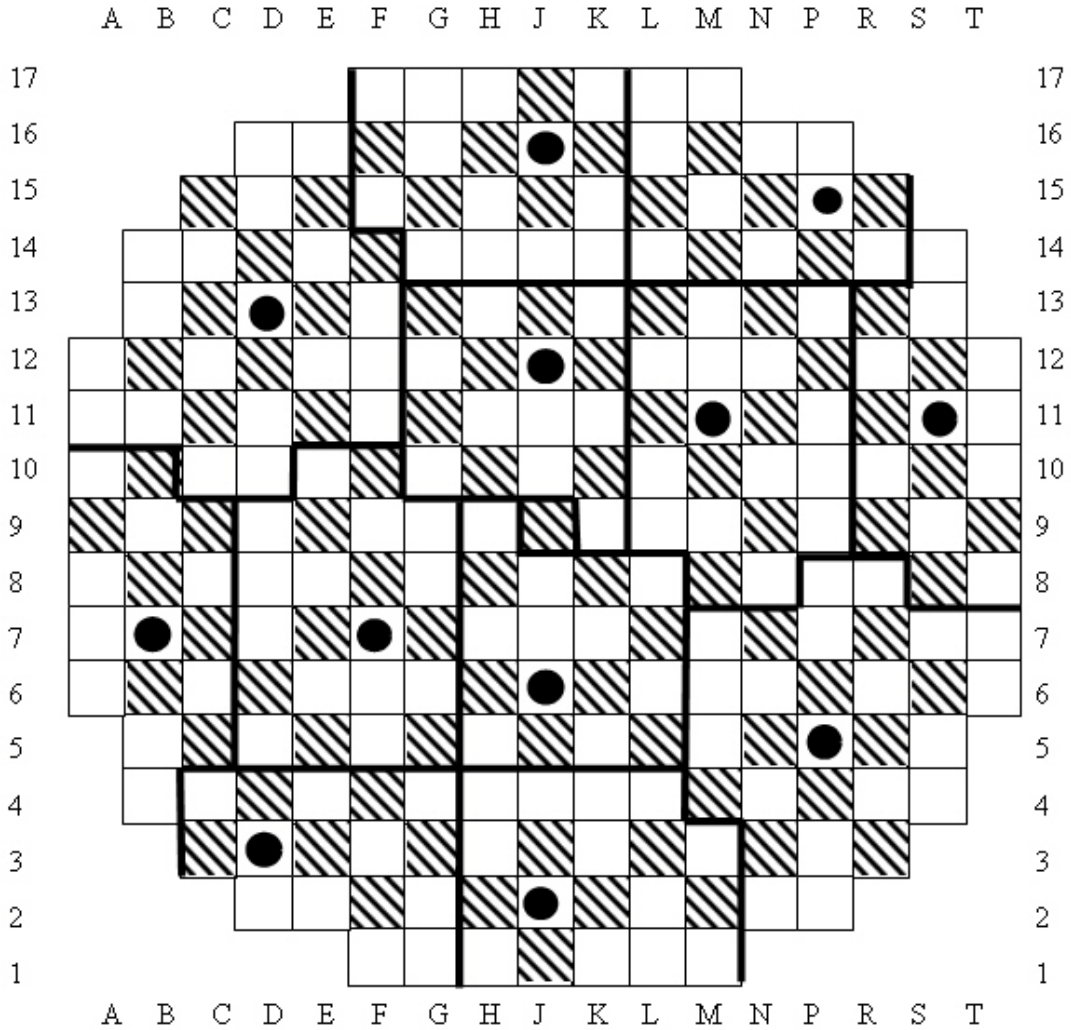
**Part Load Diagram at Mechanical Flow Rate**


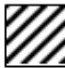





**SUB-CHAPTER 4.4 - FIGURE 5**

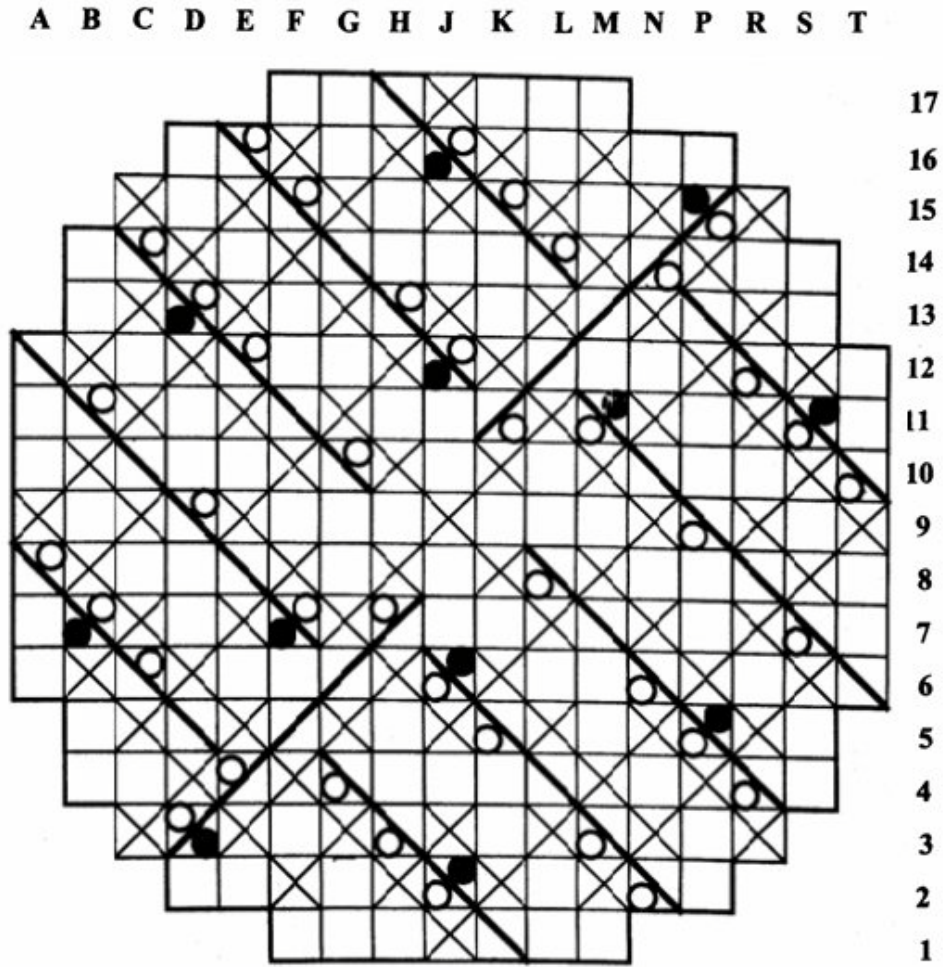
**Radial SPND Finger Locations**



-  241 FUEL ASSEMBLIES
-  89 ROD CLUSTER CONTROL ASSEMBLIES
-  12 SPND FINGERS

**SUB-CHAPTER 4.4 - FIGURE 6**

**Radial Aeroball Probe Locations**



 241 FUEL ASSEMBLIES

 89 ROD CLUSTER CONTROL ASSEMBLIES

 12 SPND FINGERS

 40 AEROBALL PROBES

## SUB-CHAPTER 4.4 – REFERENCES

External references are identified within this sub-chapter by the text [Ref-1], [Ref-2], etc at the appropriate point within the sub-chapter. These references are listed here under the heading of the section or sub-section in which they are quoted.

### 1. DESIGN BASIS

#### 1.2. FUEL TEMPERATURE DESIGN BASIS

[Ref-1] A Chotard. Melting point of UO<sub>2</sub> and (U,Gd) O<sub>2</sub> fuels. TFJC DC 906EN Revision A. AREVA . September 1997. (E)

[Ref-2] A Chotard and K Sawyer. Study on the melting point of oxide fuels and its changes with burnup. FFDC03429. AREVA . December 2006. (E)

#### 1.3. CORE FLOW DESIGN BASIS

[Ref-1] P Bertrand. RPV T/H Design : Core Bypass. NEPR-F DC 10 Revision D. AREVA. June 2008. (E)

#### 1.4. NUCLEATE BOILING

[Ref-1] Void fraction for Fuel Assembly equipped with M5® cladding tube. FS1-0000531 Revision 1.0 BPE. AREVA. March 2010. (E)

### 2. DESCRIPTION OF LIMITING PHYSICAL PHENOMENA - DESIGN CRITERIA

#### 2.2. CRITICAL HEAT FLUX RATIO OR DEPARTURE FROM NUCLEATE BOILING RATIO AND MIXING TECHNOLOGY

##### 2.2.1. Departure from nucleate boiling technology

[Ref-1] J P Bourteele. FC - FRAMATOME Critical Heat Flux correlation for AFA-2G and AFA-3G fuel assemblies description. EPD DC 511 Revision A . AREVA. April 2001. (E)

[Ref-2] L S Tong, Y S Tang. Boiling Heat Transfer and Two-Phase Flow. ISBN-13: 9781560324850. Taylor & Francis (CRC Press). 2007. (E)

**2.2.4. Manufacturing uncertainties**

[Ref-1] S Laurent. EPR - FA3 NSSS Operating Parameters. NFPSC DC 1042 Revision C. AREVA. December 2006. (E)

**2.2.5. Effects of in-pile rod bow on critical heat flux**

[Ref-1] S Laurent. EPR - FA3 NSSS Operating Parameters. NFPSC DC 1042 Revision C. AREVA. December 2006. (E)

**2.2.6. Effect of crud deposition**

[Ref-1] Status on Crud Monitoring and Acceptability. FS1-0001318 Revision 1.0. AREVA. July 2010. (E)

**2.2.7. Critical heat flux at the edge of the Fuel Assemblies**

[Ref-1] F Filhol. UK EPR Reactor - CHF in Peripheral Region. FS1-0001366 Revision 2.0. AREVA. July 2010. (E)

**2.6. REACTOR VESSEL AND CORE HYDRAULICS****2.6.1. Bypass flow**

[Ref-1] P Bertrand. RPV T/H Design: Core Bypass. NEPR-F DC 10 Revision D. AREVA. June 2008. (E)

**2.6.2. Core inlet flow maldistribution**

[Ref-1] M N Jullion. Qualification Report - FLICA III-F Version 3. NFPSC DC 188 Revision A. AREVA. January 2006. (E)

**2.6.3. Core vessel pressure drops**

[Ref-1] S Laurent. EPR - FA3 NSSS Operating Parameters. NFPSC DC 1042 Revision C. AREVA. December 2006. (E)

**3. OPERATING THERMAL AND HYDRAULIC REACTOR PARAMETERS****3.1. TEMPERATURE POWER OPERATING MAP**

[Ref-1] S Laurent. EPR - FA3 NSSS Operating Parameters. NFPSC DC 1042 Revision C. AREVA. December 2006. (E)

**SUB-CHAPTER 4.4 - TABLES 1 AND 2**

**[Ref-1]** S Laurent. EPR - FA3 NSSS Operating Parameters. NFPSC DC 1042 Revision C. AREVA. December 2006. (E)

**[Ref-2]** P Bertrand. RPV T/H Design : Core Bypass. NEPR-F DC 10 Revision D. AREVA. June 2008. (E)